# Evidence for decadal variation in global terrestrial evapotranspiration between 1982 and 2002: 1. Model development

Kaicun Wang,[1,2,3] Robert E. Dickinson,[2] Martin Wild,[4] and Shunlin Liang[1]

Received 15 December 2009; revised 26 July 2010; accepted 6 August 2010; published 23 October 2010.

[1] Estimating interannual to decadal variability of terrestrial evapotranspiration (ET) requires use of standard meteorological data complemented with some high-resolution satellite data. A semiempirical expression for this purpose is developed and validated with data from 2000 to 2007. These data were collected at 64 globally distributed sites, including the continuous measurements collected by the Atmospheric Radiation Measurement (ARM) and FLUXNET projects, and are the longest available, with continuous worldwide multisite measurements of ET, and a total of 274 site years. The sites are mainly located in North America and Asia, with the exception of three sites in Australia, two in Europe, and one in Africa. The climates of the sites vary from tropical to subarctic and from arid to humid. The land cover types of the sites vary from desert, croplands, grasslands, and shrub land to forests. On average, the 16 day average daily ET can be estimated with an error (standard deviation) of 17 W m$^{-2}$ (25% in relative value), and with an average correlation coefficient of 0.94. The standard deviation of the comparison between measured and predicted site-averaged daily ET is 9 W m$^{-2}$ (14%), with a correlation coefficient of 0.93. The model is also satisfactory in reproducing the interannual variability at sites with 5 years of data in both humid and arid regions. The correlation coefficient between measured and predicted annual ET anomalies is 0.85. This simple but accurate method permits us to investigate decadal variation in global ET over the land as will be demonstrated in part two of this paper series.

**Citation:** Wang, K., R. E. Dickinson, M. Wild, and S. Liang (2010), Evidence for decadal variation in global terrestrial evapotranspiration between 1982 and 2002: 1. Model development, *J. Geophys. Res.*, *115*, D20112, doi:10.1029/2009JD013671.

## 1. Introduction

[2] Terrestrial evapotranspiration (ET) is central to earth system science and its constitutive cycles (water, energy, and biogeochemical). Many aspects of hydrology, climate and weather prediction depend upon accurate determination of ET. The U.S. National Research Council's "Decadal Survey" [*National Research Council*, 2007] views the accurate estimation of ET to be a major challenge. Since the 1990s, ET measurements have been collected at tower sites. However, the current eddy covariance or Bowen ratio systems at tower sites [*Baldocchi et al.*, 2001; *National Research Council*, 2007] have three limitations: (1) the tower density is too low to adequately measure ET variation at the local, national, and global scale, (2) these systems are too expensive to run routinely at a reasonable density at the global scale, and (3) data is only available from the 1990s onward.

[3] An alternative approach, the Penman-Monteith equation, can be accurate where net radiation and stomatal resistance is available and the vegetation is not water stressed. Various other algorithms make use of recent satellite data, i.e., available since 2000. However, none of the available approaches can be used for monitoring global ET on decadal scales for lack of needed data. The point of this paper is to provide an approach that provides global ET over several decades. For this purpose, we use a model structure patterned after that of the equation of *Penman* [1948], i.e.,

$$\lambda E = ET = ET_E + ET_A = \frac{\Delta}{\Delta + \gamma} \cdot (R_n - G) + \frac{\gamma}{\Delta + \gamma} \cdot VPD \cdot g_a, \quad (1)$$

where $\Delta = de^*/dt$ is the gradient of the saturated vapor pressure ($e^*$) to the air temperature ($T_a$), and $\gamma$ is the psychrometric constant, $R_n$ is surface net radiation, $G$ is ground heat flux, VPD is the water vapor pressure deficit (i.e., departure from saturation) and $g_a$ is aerodynamics conductance. The factors $\Delta/(\Delta + \gamma)$ and $\gamma/(\Delta + \gamma)$ in equation (1)

[1]Department of Geography, University of Maryland, College Park, Maryland, USA.
[2]Department of Geological Sciences, University of Texas at Austin, Austin, Texas, USA.
[3]College of Global Change and Earth System Science, Beijing Normal University, Beijing, China.
[4]Institute for Atmospheric and Climate Science, ETH Zurich, Zurich, Switzerland.


0148-0227/10/2009JD013671

depend solely on $T_a$ at a given location [*Wang et al.*, 2006]. VPD can be calculated from conventional meteorological observations of $T_a$ and relative humidity (RH). The first term on the right-hand side of the equation represents the energy control on ET ($ET_E$) and the second term represents the atmospheric control ($ET_A$).

[4] A large number of past empirical approaches have been built around the physical principles embodied in equation (1). In particular, *Priestley and Taylor* [1972] showed under some conditions, that ET could be estimated with only the first, energy control term, multiplied by an empirical factor. Other authors address the issue of control by soil moisture [*Davies and Allen*, 1973; *Koster and Suarez*, 1999; *Komatsu*, 2003; *Burba and Verma*, 2005; *Detto et al.*, 2006; *Li et al.*, 2006; *Granier et al.*, 2007; *Phillips et al.*, 2009], but the required soil moisture data for such treatment is not globally available [*Entin et al.*, 1999; *Robock et al.*, 2003; *Dirmeyer et al.*, 2004; *Gao and Dirmeyer*, 2006; *Schaake et al.*, 2004].

[5] *Monteith* [1965] modified equation (1) to include the control of stomatal resistance on ET, another parameter that is not globally available. During the last decade, a large number of techniques have been proposed to estimate ET from satellite observations (see *Wang et al.* [2007] and *Kalma et al.* [2008] for further review). The methods that use the surface-air temperature gradient require unbiased land surface temperature ($T_s$) retrievals and air temperature ($T_a$) interpolated from ground-based point measurements. Such methods are sensitive to errors in $T_s$ or $T_a$ [*Timmermans et al.*, 2007]. Spatial and temporal variation of $T_s$ is used to reduce the sensitivity [*Anderson et al.*, 1997; *Wang et al.*, 2006]. Furthermore, satellite $T_s$ retrievals are only available under clear sky conditions and for a limited period of time. Most existing methods using satellite observations to estimate ET do not directly consider the role of a deficit in air humidity.

[6] The currently most accurate available ET measurements alone do not provide estimates of ET with high spatial resolution and long history. However, they can be used to develop an approach, patterned after equation (1) and using conventional meteorological observations and some satellite data. Equation (1) has three deficiencies that preclude its direct use for our intended purpose: (1) it requires $R_n$ that is not widely available; (2) it neglects any soil moisture stress; and (3) it neglects the controls of vegetation on ET.

[7] By analyzing long-term ET measurements collected by the Atmospheric Radiation Measurements (ARM) project, *Wang et al.* [2007] found that the dominant parameters controlling ET are surface net radiation ($R_n$), temperature either as air temperature ($T_a$) or land surface temperature ($T_s$), and vegetation cover quantified by vegetation indices (VI). Recently, numerous studies have related ET to VIs for various land cover types and different regions of the world [*Burba and Verma*, 2005; *Detto et al.*, 2006; *Li et al.*, 2006; *Nagler et al.*, 2005; *Blyth et al.*, 2006; *Min and Lin*, 2006; *Yang et al.*, 2006; *Schüttemeyer et al.*, 2007; *Watts et al.*, 2007; *Hammerle et al.*, 2008]. In particular, *Choudhury et al.* [1994] related the ratio of *ET* to potential evaporation to VIs. *Schüttemeyer et al.* [2007] further developed a method to estimate ET by multiplying the first term of equation (1) by VF where VF is a linear function of VI, i.e., providing a simple dependence of variations of ET on the vegetation.

[8] This first part of the two-part paper develops a semi-empirical method for estimating ET. Although likely to be much less accurate instantaneously than direct measurements or the Penman-Monteith equation, it provides stable long-term statistics, as needed to examine interannual and decadal variability globally. Since it makes use of essentially all the data that are available for this purpose, any other competitive method would have to use the same data or a subset thereof.

## 2. Model Development

[9] Satellite terrestrial observations can supply global vegetation conditions at high temporal and spatial resolution [*Tucker et al.*, 1985]. Two kinds of VIs have been widely accepted: normalized difference vegetation index (NDVI) and enhanced vegetation index (EVI) derived from satellite data, such as Moderate Resolution Imaging Spectroradiometer (MODIS) and Advanced Very High Resolution Radiometer (AVHRR) [*Huete et al.*, 2002].

$$NDVI = (\rho_{nir} - \rho_{red})/(\rho_{nir} + \rho_{red}) \quad (2)$$

$$EVI = 2.6 \times (\rho_{nir} - \rho_{red})/(\rho_{nir} + 6 \times \rho_{red} + 7.5 \times \rho_{blue} + 1.0), \quad (3)$$

where $\rho$ is the reflectance after atmospheric correction, the subscript of "nir" indicates the near-infrared band, "red" is the red band and "blue" is the blue band.

[10] NDVI characterizes vegetation cover density and type [*Tucker et al.*, 1985]. NDVI varies from 0 to 1 for terrestrial surfaces excluding snow/ice and water surfaces; the higher the value, the denser the vegetation. NDVI loses sensitivity to vegetation coverage (or leaf area) when the vegetation is dense. The EVI is designed to correct the saturation problem of NDVI, and is available from the new generation satellite data, such as MODIS. Figure 1 shows that EVI increases at a higher rate than NDVI when the vegetation indices are relatively high, indicating EVI from MODIS at least partly corrects the saturation problem of NDVI. However, it is only available after 2000. Therefore, in this study, we create models for both NDVI and EVI to estimate long-term variations of ET.

[11] Over a day, aerodynamic conductance can be parameterized as a linear function of daily wind speed (WS) [*Shuttleworth*, 1993; *Parlange et al.*, 1995; *Shuttleworth*, 2007],

$$g_a = a \cdot (1 + b \cdot WS). \quad (4)$$

Since equation (4) ignores the influence of stability on aerodynamics and its use on an hourly time scale is not advised. In this study, we use the relative humidity deficit (RHD) as an index of soil water deficit to quantify the dependence of ET on soil water stress [*Mu et al.*, 2007],

$$RHD = 1 - RH/100, \quad (5)$$

where RH is relative humidity in unit of %.

[12] Equation (1) and the preceding paragraphs suggest the following form to be used in this study:

$$ET = \frac{\Delta}{\Delta + \gamma \cdot} \cdot (R_n - G) \cdot g_s + \frac{\gamma}{\Delta + \gamma} \cdot VPD \cdot g_a \cdot g_s, \quad (6)$$

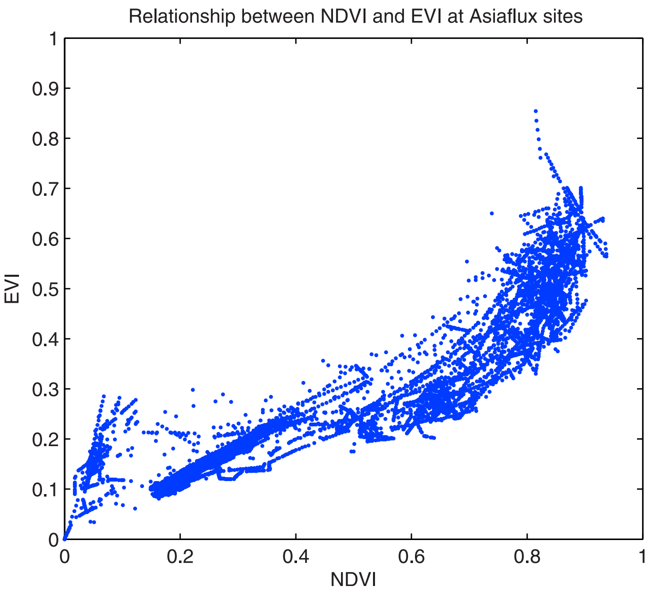


**Figure 1.** An example of the nonlinear relationship between MODIS NDVI and EVI. The data are from 2001 to 2007 at the sites in Asia shown in Table 1. NDVI loses sensitivity to vegetation coverage (or leaf area) when vegetation is dense. EVI is designed to correct the saturation problem of NDVI. This plot shows that EVI increases at higher rate than NDVI when the vegetation indices are relative high, indicating EVI at least partly correct the saturation problem of NDVI.

where

$$g_s \approx A + RHD \cdot (B + C \cdot VI). \quad (7)$$

According to *Jarvis* [1976], $g_s$ mainly depends on soil moisture (SM), leaf area (quantified by VI here), $T_a$, and incident solar radiation ($R_s$). SM is diagnosed by the RHD term and the latter two terms are directly included.

[13] Therefore, equation (1) is modified to

$$ET_E = \frac{\Delta}{\Delta + \gamma} \cdot R_s \cdot [a_1 + a_2 \cdot VI + RHD \cdot (a_3 + a_4 \cdot VI)], \quad (8)$$

$$ET_A = \frac{\gamma}{\Delta + \gamma} \cdot WS \cdot VPD \cdot [a_5 + RHD \cdot (a_6 + a_7 VI)], \quad (9)$$

$$ET = a_8 \cdot (ET_E + ET_A) + a_9 \cdot (ET_E + ET_A)^2, \quad (10)$$

where the VI can be NDVI or EVI. The nonlinear form of equation (10) is selected to address the saturation issues of NDVI shown in Figure 1. NDVI loses sensitivity to vegetation coverage (or leaf area) when vegetation is dense and EVI effectively corrects the saturation effect of NDVI [*Huete et al.*, 2002] (see also Figure 1). When EVI is used in equations (8)–(10), the nonlinear item ($a_9$) is negligible and then equation (10) is equal to traditional Penman-Monteith Equation ($ET = ET_A + ET_E$, as in equation (1)).

[14] A crucial difference between equations (8)–(10) and past formulations is they use $R_s$ rather than $R_n$ because $R_n$ is not conventionally observed and its current satellite estimates are not sufficiently accurate for this purpose. A previous study [*Wang and Liang*, 2009] found that the ratio $R_n$ to $R_s$ has a substantial seasonal variation. Factors that control this variation are: (1) atmospheric downward longwave radiation changes with seasonal variation in air temperature and atmospheric water vapor content, especially near the surface; and (2) surface longwave emission varies in response to the cooling effect of ET. The ratio of $R_n$ to $R_s$ can be accurately parameterized by a linear function of VI, $T_a$ and RH (that quantify the dependence on water vapor content and cloud cover); that is, daytime $R_n$ can be estimated from $R_s$ with the addition of $T_a$, RH and VI data for various land cover types and different surface elevations ranging from 98 m to 4700 m [*Wang and Liang*, 2009]. Therefore, the linear function of VI ($a_2$) that is added into equation (8) helps account for the impact of vegetation in determining the ratio of $R_n$ to $R_s$.

[15] The coefficients ($a_1$-$a_9$) are derived by regression and validated using ground-based measurements that are explained in detail in section 3. Stomatal conductance is parameterized as a linear function of VIs and RHD (i.e., as incorporated in equation (8)) and aerodynamic conductance is parameterized as a linear function of WS (i.e., equation (4)). Vegetation height may influence the impact of stomatal conductance, and we tried to parameterize this effect by adding a logarithmic function of vegetation height to equation (7); however, our regression results indicated that the climatological variability of ET explained by vegetation height is very small, as also reported by *Blyth et al.* [2006]. Because most ET occurs in daytime, daytime averaged $R_s$ is used in equation (8) and the ET calculated from equations (10) is also a daytime average. Results are represented as daily values by converting daytime ET to its daily value, i.e., multiplying ET by day length (in hours) and then dividing by 24 h.

[16] A major advantage of equations (8)–(10) is that they avoid using the temperature or humidity differences that are used by many of the remote sensing methods to estimate ET [*Wang et al.*, 2007]. Consequently the sensitivity of this parameterization to errors in the input data is substantially lessened [*Wang et al.*, 2007; *Wang and Liang*, 2008]. Another advantage is that it requires only easily obtainable measurements. Reliable long-term SM estimates that is needed to parameterize ET in previous methods are not available at global and regional scales [*Gao and Dirmeyer*, 2006; *Reichle et al.*, 2004; *Wagner et al.*, 2003]. Section 3 shows that the proposed method can accurately predict global ET over a range of land cover types and climates, for both seasonal and annual variations in ET.

## 3. Validation Data

[17] The method is validated with a large data set of ground-based measurements, including the long-term measurements collected by Ameriflux, Asiaflux, and Atmospheric Radiation Measurement (ARM) program, and additional sites operated by individual principal investigators released by the FLUXNET website. These data sets include the longest continuous worldwide multisite measurements of ET, $R_s$, and corresponding meteorological observations. The data were collected at 64 sites, and provide a data set with a total length of 274 years. The sites are mainly located in North America and Asia, with three sites in Australia, two sites in Europe, and one site in Africa (Figure 2 and Table 1). The climate of the sites ranges from tropical to arctic and arid to humid.

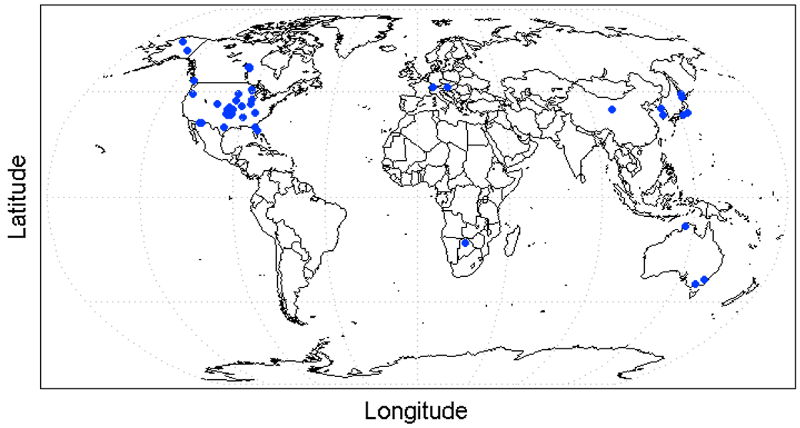


**Figure 2.** Location of the 64 sites used in this study.

Elevation ranges from near sea surface level to more than 3000 m above sea level (Table 1). The land cover types of the sites include desert grasslands, rainfed and irrigated croplands, grazed and ungrazed grasslands, savanna, shrub land, deciduous forest, evergreen forest and mixed forests (Table 1).

[18] The ET measurements are collected by two widely accepted methods: The Energy Balance Bowen Ratio (EBBR) method and the Eddy COvaRiance (ECOR) method. The EBBR method was used by the ARM project to collect ET data at fourteen sites over the Southern Great Plains of the United States since 1995 and the Solar and Infrared Radiation Station (SIRS) system collected the surface energy components since 2002. The ECOR method was used to collect the ET data from the Ameriflux, Asiaflux and the research sites operated by individual investigators (Table 1). The ECOR method is accepted as the best method to directly measure heat fluxes and is widely used in global measurement experiments such as FLUXNET [*Baldocchi et al.*, 2001]. However, this method does not conserve energy; that is, it has an energy closure ratio $R_a$ that is for the global FLUXNET measurements of about 0.8 [*Wilson et al.*, 2002], where $R_a$ is

$$R_a = \frac{ET_{EC} + H_{EC}}{R_n - G}, \tag{11}$$

and where $ET_{EC}$ and $H_{EC}$ are the original ET and sensible heat flux ($H$) measured by the ECOR method, and $G$ is the ground heat flux. Evidently, ET or $H$ or both must be substantially underestimated since $R_a$ should be equal to unity according to the conservation of energy principle. Although several reasons have been proposed to explain this energy imbalance [*Wilson et al.*, 2002; *Gao*, 2005; *Oncley et al.*, 2007], its mechanism remains unclear [*Oncley et al.*, 2007]. *Twine et al.* [2000] proposed a method to correct this discrepancy by assuming the Bowen ratio (the ratio of $H$ to ET) measured by ECOR is fixed, i.e.,

$$ET = \frac{ET_{EC}}{R_a} \tag{12}$$

$$H = \frac{H_{EC}}{R_a}. \tag{13}$$

[19] MODIS global 16 day averaged EVI and NDVI data (https://wist.echo.nasa.gov/api/) are used in this study because we found that the EVI is a better factor in parameterizing ET. However, EVI is not available before 2000 when MODIS data became available. To investigate long-term variability of ET, we will use AVHRR NDVI data in the second part of this two-part paper [*Wang et al.*, 2010]. MODIS NDVI and EVI corresponding to the time period show in Table 1 are used in this study.

## 4. Model Validation

[20] We use data of the first 15 sites in Table 1 to derive the coefficients in equations (8)–(10) and data from the other sites to validate the method. Such sites are located in homogeneous areas. The derived coefficients are summarized in Table 2. After obtaining coefficients from the regression, equations (8)–(10) are used to estimate ET for each site with the same coefficients and the results are compared with ground-based measurements of ET.

[21] A comparison of our validation results with those of our previous studies [*Wang et al.*, 2007; *Wang and Liang*, 2008] indicates that the atmosphere control terms (the last three terms) improve the parameterization of ET although their contributions are much less than the energy terms, presumably because humidity will adjust to ET through boundary layer processes on daily and longer time scales. However, the terms may be very important in study of long-term variations [*Wang et al.*, 2010].

[22] The comparison of the measured and predicted 16 day average daily ET when *EVI* is used at all 64 sites demonstrates that equations (8)–(10) accurately predict seasonal ET (Figure 3). On average, the 16 day average daily ET is predicted with an error (standard deviation) of 17.1 W m$^{-2}$ (25.3% in relative value). The correlation coefficient is 0.93 averaged over the 64 sites. We used the 16 day average because the MODIS EVI data are available for 16 day intervals. Table 3 summarizes the statistical parameters for all sites.

[23] The results are similar when NDVI is used (Figure 4 and Table 3). The 16 day average daily ET estimated with NDVI has an error (standard deviation) of 17.0 W m$^{-2}$

**Table 1.** A Summary of the Information for the 64 Sites Used in This Study[a]

| Site Name | Land Cover | NDVI | Std NDVI | Lat | Lon | Elev | ET | $T_a$ | $R_H$ | $R_n$ | $R_s$ | Year | Method |
|---|---|---|---|---|---|---|---|---|---|---|---|---|---|
| KoFlux Gwangneung Supersite | Mixed deciduous/coniferous forest | 0.80 | 0.09 | 37.75 | 127.15 | 340 | 222.5 | 25.9 | 61 | 364.5 | 449.4 | 2005–2006 | ECOR |
| KoFlux Haenam site | Rice/farm land | 0.61 | 0.17 | 34.92 | 126.95 | 14 | 136.6 | 14.7 | 53 | 280.2 | 475.8 | 2004–2006 | ECOR |
| Mase paddy flux site | Rice paddy field | 0.44 | 0.13 | 36.05 | 140.03 | 13 | 195.2 | 16.5 | | 320.2 | 442.5 | 2001–2001 | ECOR |
| Tomakomai Flux Research Site | Japanese larch forest | 0.64 | 0.22 | 42.74 | 141.52 | 140 | 112.9 | 8.8 | 64 | 278.7 | 384.6 | 2002–2004 | ECOR |
| Kendall | Desert grasslands | 0.22 | 0.07 | 31.74 | -109.94 | 1526 | 54.9 | 20.5 | 31 | 367.3 | 599.6 | 2000–2007 | EBBR |
| Lucky Hills | Desert Shrubland | 0.21 | 0.06 | 31.74 | -110.05 | 1372 | 53.8 | 21.6 | 30 | 361.4 | 605.4 | 2000–2007 | EBBR |
| Moshiri-Birch | Deciduous broadleaf Forest | 0.60 | 0.34 | 44.39 | 142.32 | 585 | 125.3 | 9.3 | 80 | 260.2 | 395.1 | 2003–2006 | ECOR |
| Seto-Mixed | Mixed evergreen/deciduous Forest | 0.74 | 0.12 | 35.26 | 137.08 | 205 | 161.3 | 15.1 | 57 | 322.7 | 450.0 | 2002–2006 | ECOR |
| Howard Springs | Savanna/tropical | 0.57 | 0.15 | −12.50 | 131.15 | 79 | 248.7 | 29.8 | 57 | 424.7 | 577.6 | 2001–2006 | ECOR |
| Tumbarumba | Forest | 0.73 | 0.12 | −35.66 | 148.15 | 700 | 163.6 | 12.0 | 59 | 358 | 531.9 | 2001–2006 | ECOR |
| Wallaby Creek Melbourne | Temperate forest | 0.81 | 0.03 | −37.43 | 145.19 | 685 | 156.4 | 13.0 | 65 | 351.5 | 375.4 | 2005–2007 | ECOR |
| Wallaby Creek canopy Melbourne | Temperate forest | 0.8 | 0.03 | −37.43 | 145.19 | 685 | 112.1 | 14.1 | 62 | 256.7 | 356.7 | 2005–2007 | ECOR |
| Maun Botswana Africa | Mopane woodland | 0.36 | 0.10 | −19.92 | 23.59 | 900 | 107.5 | 25.6 | 37 | 386.3 | 561.0 | 2000–2001 | ECOR |
| British Columbia Campbell River | Evergreen needleleaf/boreal Forest | 0.81 | 0.15 | 49.87 | −125.33 | 300 | 95.0 | 10.9 | 77 | 247.8 | 333.0 | 2000–2002 | ECOR |
| UCI - 1930 burn site Canada | Evergreen needleleaf/boreal Forest | 0.54 | 0.21 | 55.91 | −98.52 | 260 | 50.3 | 8.7 | 61 | 223.3 | 315.1 | 2001–2005 | ECOR |
| UCI - 1850 burn site Canada | Evergreen needleleaf/boreal Forest | 0.55 | 0.22 | 55.88 | −98.48 | 260 | 46.4 | 6.4 | 63 | 224.4 | 317.3 | 2002–2005 | ECOR |
| UCI - 1964 burn site Canada | Evergreen needleleaf/boreal Forest | 0.45 | 0.25 | 55.91 | −98.38 | 260 | 44.4 | 2.3 | 62 | 219.3 | 320.6 | 2001–2005 | ECOR |
| UCI - 1981 burn site Canada | Evergreen needleleaf/boreal Forest | 0.52 | 0.24 | 55.86 | −98.49 | 260 | 52.5 | 4.8 | 62 | 222.4 | 329.4 | 2001–2005 | ECOR |
| UCI - 1989 burn site Canada | Evergreen needleleaf/boreal Forest | 0.42 | 0.26 | 55.92 | −98.96 | 260 | 39.5 | 2.6 | 62 | 179.9 | 313.1 | 2001–2005 | ECOR |
| UCI - 1998 burn site Canada | Evergreen needleleaf/boreal Forest | 0.37 | 0.27 | 55.92 | −98.96 | 260 | 53.5 | 5.6 | 59 | 187.4 | 320.8 | 2002–2005 | ECOR |
| Seebodenalp Switzerland | Mixed forest | 0.69 | 0.23 | 47.07 | 8.47 | 1025 | 142.4 | 10.5 | 76 | 230.7 | 348.5 | 2002–2005 | ECOR |
| Haibei China | Grasslands | 0.39 | 0.25 | 37.60 | 101.30 | 3250 | 82.4 | 3.0 | 50 | 265.3 | 483.7 | 2002–2004 | ECOR |
| Hillsboro, Kansas: EF02 | Grass | 0.47 | 0.11 | 38.31 | −98.30 | 447 | 138.3 | 16.0 | 61 | 270.9 | 466.3 | 2002–2006 | ECOR |
| Plevna, Kansas: EF04 | Rangeland (ungrazed) | 0.4 | 0.13 | 37.95 | −98.33 | 513 | 97.6 | 14.9 | 60 | 279.5 | 441.5 | 2002–2006 | EBBR |
| Elk Falls, Kansas: EF07 | Pasture | 0.55 | 0.14 | 37.38 | −96.18 | 283 | 156.4 | 16.7 | 64 | 269.4 | 461.2 | 2002–2006 | EBBR |
| Coldwater, Kansas: EF08 | Rangeland | 0.35 | 0.10 | 37.33 | −99.31 | 664 | 113.5 | 16.5 | 59 | 295.8 | 471.5 | 2002–2006 | EBBR |
| Ashton, Kansas: EF09 | Pasture | 0.44 | 0.10 | 37.13 | −97.27 | 386 | 134.4 | 16.4 | 61 | 274.9 | 458.1 | 2002–2006 | EBBR |
| Pawhuska, Oklahoma: EF12 | Native prairie | 0.53 | 0.19 | 36.84 | −96.43 | 331 | 139.3 | 17.1 | 63 | 286.5 | 454.2 | 2002–2006 | EBBR |
| Lamont, Oklahoma: EF13 | Pasture and wheat | 0.45 | 0.10 | 36.61 | −97.49 | 318 | 135.4 | 17.9 | 59 | 286.5 | 467.9 | 2002–2006 | EBBR |
| Ringwood, Oklahoma: EF-15 | Pasture | 0.43 | 0.13 | 36.43 | −98.28 | 418 | 111.8 | 15.6 | 58 | 265.2 | 458.2 | 2002–2006 | EBBR |
| Morris, Oklahoma: EF-18 | Pasture | 0.52 | 0.14 | 35.69 | −95.86 | 217 | 154.2 | 19.0 | 63 | 283.6 | 465.8 | 2002–2006 | EBBR |
| El Reno, Oklahoma: EF-19 | Pasture (ungrazed) | 0.5 | 0.15 | 35.56 | −98.02 | 421 | 145.6 | 18.3 | 59 | 305.6 | 482.9 | 2002–2006 | EBBR |
| Meeker, Oklahoma: EF-20 | Pasture | 0.49 | 0.13 | 35.56 | −96.99 | 309 | 138 | 18.1 | 60 | 285.0 | 458.7 | 2002–2006 | EBBR |
| Cordell, Oklahoma: EF-22 | Rangeland (grazed) | 0.38 | 0.07 | 35.35 | −98.98 | 465 | 125.3 | 18.2 | 55 | 292.6 | 475 | 2002–2006 | EBBR |
| Cement, Oklahoma: EF26 | Pasture | 0.48 | 0.09 | 34.96 | −98.08 | 400 | 140.8 | 19.4 | 59 | 301.5 | 480.7 | 2002–2006 | EBBR |
| Earlsboro, Oklahoma:EF27 | Pasture | 0.5 | 0.13 | 35.27 | −96.74 | 300 | 144.5 | 18.3 | 59 | 287.8 | 468.6 | 2003–2006 | EBBR |
| Palangkaraya | Evergreen broadleaf forest | 0.62 | 0.26 | 46.96 | 16.65 | 248 | 256.7 | 29.2 | 67 | 463.4 | 558.4 | 2002–2003 | EBBR |
| Tomakomai National Forest | Forest | 0.66 | 0.19 | 42.74 | 141.52 | 140 | 106.6 | 8.6 | 67 | 252.7 | 351.4 | 2001–2003 | ECOR |
| Ivotuk | Open shrub lands | 0.33 | 0.29 | 68.49 | −155.75 | 1650 | 41.6 | 0.4 | 76 | 117.0 | 292.6 | 2003–2006 | ECOR |
| Audubon Research Ranch | Savanna/temperate | 0.25 | 0.09 | 31.59 | −110.51 | 985 | 71.3 | 21.1 | 33 | 268.2 | 567.7 | 2002–2006 | ECOR |
| Kendall Grasslands | Grasslands | 0.22 | 0.08 | 31.74 | −109.94 | 1531 | 57.6 | 19.9 | 29 | 313.9 | 588.5 | 2004–2006 | ECOR |
| Santa Rita Mesquite | Savanna | 0.24 | 0.06 | 31.82 | −110.87 | 1120 | 72.6 | 22.5 | 27 | 337.0 | 560.6 | 2004–2006 | ECOR |
| Bonanza creek 1987 burn Delta | Forest | 0.43 | 0.22 | 63.92 | −145.38 | 900 | 57.6 | 6.1 | 55 | 162.1 | 298.8 | 2003–2003 | ECOR |
| Bonanza creek 1999 burn Delta Junction | Grassland | 0.45 | 0.21 | 63.92 | −145.38 | 900 | 55.0 | 6.4 | 54 | 172.2 | 288.2 | 2003–2003 | ECOR |
| Bonanza creek control Delta Junction | Forest | 0.41 | 0.23 | 63.92 | −145.38 | 900 | 56.0 | 4.9 | 54 | 205.5 | 269.1 | 2003–2003 | ECOR |
| Goodwin Creek | Deciduous broadleaf forest/temperate | 0.64 | 0.15 | 34.25 | −89.97 | 70 | 164.7 | 20.5 | 68 | 277.2 | 452.7 | 2002–2006 | ECOR |

**Table 1.** (continued)

| Site Name | Land Cover | NDVI | Std NDVI | Lat | Lon | Elev | ET | $T_a$ | $R_H$ | $R_n$ | $R_s$ | Year | Method |
|---|---|---|---|---|---|---|---|---|---|---|---|---|---|
| Fermi Laboratory (agricultural) Batavia | Croplands (Corn -C4/Soybean - C3) | 0.51 | 0.22 | 41.86 | −88.23 | 227 | 134.2 | 14.2 | 61 | 243.0 | 418.7 | 2005–2007 | ECOR |
| Fermi Laboratory (prairie) Batavia | Grassland | 0.46 | 0.24 | 41.84 | −88.24 | 227 | 147.4 | 13.0 | 63 | 262.8 | 390.5 | 2004–2007 | ECOR |
| Bondville | Croplands | 0.44 | 0.23 | 40.01 | −88.29 | 300 | 143.4 | 15.3 | 68 | 262.8 | 435.5 | 2000–2007 | ECOR |
| Kennedy Space Center (scrub oak) | Evergreen broadleaf/tropical | 0.71 | 0.12 | 28.61 | −80.67 | 5 | 204.7 | 24.2 | 65 | 361.5 | 485.7 | 2000–2006 | ECOR |
| Mead irrigated continuous maize | Crops (Corn - C4/Soybean - C3) | 0.43 | 0.21 | 41.17 | −96.48 | 361 | 133.2 | 13.3 | 64 | 255.9 | 418.1 | 2001–2005 | ECOR |
| Mead irrigated maize-soybean rotation | Crops (Corn - C4/Soybean - C3) | 0.43 | 0.2 | 41.16 | −96.47 | 361 | 129.1 | 12.8 | 66 | 252.7 | 417.7 | 2001–2005 | ECOR |
| Mead - rainfed maize-soybean rotation | Crops (Corn - C4/Soybean - C3) | 0.42 | 0.21 | 41.18 | −96.44 | 361 | 126.3 | 13.4 | 63 | 251.6 | 415.1 | 2001–2005 | ECOR |
| Metolius - intermediate aged ponderosa pine | Evergreen needleleaf/temperate | 0.61 | 0.14 | 44.45 | −121.56 | 1310 | 84.1 | 9.3 | 56 | 271.7 | 420.9 | 2002–2005 | ECOR |
| Ozark | Deciduous broadleaf forest/temperate | 0.64 | 0.22 | 38.74 | −92.20 | 220 | 167.8 | 16.2 | 58 | 340.8 | 463.2 | 2004–2004 | ECOR |
| Niwot Ridge Forest | Evergreen needleleaf/temperate | 0.53 | 0.16 | 40.03 | −105.55 | 3050 | 106.2 | 4.9 | 48 | 331.3 | 465.6 | 2000–2007 | ECOR |
| Brookings | Grasslands | 0.49 | 0.23 | 44.35 | −96.84 | 510 | 175.5 | 12.0 | 67 | 268.2 | 453.3 | 2004–2006 | ECOR |
| Mize - slash pine (clear-cut 3-yr regen) | Coniferous forest | 0.67 | 0.12 | 29.76 | −82.24 | 50 | 176.5 | 23.7 | 64 | 299.8 | 434.7 | 2000–2004 | ECOR |
| Donaldson - slash pine (mid-rotation 12 yrs) | Evergreen needleleaf/tropical | 0.74 | 0.12 | 29.75 | −82.16 | 50 | 176.7 | 23.3 | 65 | 305.7 | 442.9 | 2000–2004 | ECOR |
| Walker Branch Watershed | Deciduous broadleaf/temperate | 0.62 | 0.19 | 35.96 | −84.29 | 370 | 139 | 15.9 | 60 | 332.9 | 452.5 | 2000–2007 | ECOR |
| Freeman Ranch mesquite juniper | Savanna | 0.55 | 0.11 | 29.95 | −98.00 | 272 | 128.3 | 23.6 | 51 | 315.3 | 475.6 | 2004–2006 | ECOR |
| Walnut River Watershed | Grassland | 0.49 | 0.16 | 37.53 | −96.86 | 408 | 142.5 | 16.5 | 58 | 283.6 | 466.9 | 2001–2004 | ECOR |
| Park Falls/WLEF | Evergreen needleleaf/temperate | 0.66 | 0.22 | 45.95 | −90.27 | 480 | 117.3 | 9.9 | 65 | 235.5 | 417.3 | 2000–2003 | ECOR |
| Willow Creek | Evergreen broadleaf/temperate | 0.53 | 0.30 | 45.81 | −90.08 | 520 | 97.9 | 8.1 | 80 | 256.0 | 378.3 | 2000–2006 | ECOR |

[a]Site locations are shown in Figure 1. Land cover type, vegetation index (NDVI) and its standard deviation (std NDVI) indicating variation of the seasonal vegetation coverage, latitude (Lat), longitude (Lon) and Elevation (Elev, m) are given. The multiyear averaged daytime values of ET (W m$^{-2}$), air temperature ($T_a$, °C), relative humidity (RH, %), surface net radiation ($R_n$, W m$^{-2}$), and solar radiation ($R_s$, W m$^{-2}$) are also listed. We also supplied information on the ET measured methods (EBBR: and ECOR) and the data collection dates.

**Table 2.** Coefficients in Equations (8)–(10) for the EVI and NDVI Vegetation Indices

| | EVI | NDVI |
|---|---|---|
| $a_1$ | 0.504 | 0.476 |
| $a_2$ | 0.364 | 0.284 |
| $a_3$ | −0.760 | −0.654 |
| $a_4$ | 0.855 | 0.264 |
| $a_5$ | 2.99 | 3.06 |
| $a_6$ | −3.25 | −3.86 |
| $a_7$ | 7.73 | 3.64 |
| $a_8$ | 1.000 | 0.819 |
| $a_9$ | $0.6 \times 10^{-3}$ | $1.7 \times 10^{-3}$ |

(25.1% in relative value). The correlation coefficient is also 0.94 averaged over the 64 sites. NDVI, unlike EVI, saturates when vegetation is dense. The nonlinear effect ($a_9$) of equation (10) is larger when NDVI is used in equations (8)–(10) than that of EVI. However, the differences in results are not substantial after the nonlinear term is included in equation (10) (Figures 3 and 4 and Table 3).

[24] Because EVI is less dependent on soil background, the averaged absolute value of the biases is 7.0 W m$^{-2}$ (10.5% in relative value), which is slightly better than 7.3 W m$^{-2}$ (10.9% in relative values) when NDVI is used in equations (8)–(10). The bias is less important because this study uses ET data collected by both EBBR and ECOR methods and they may be substantially different. The ARM project deploys the EBBR and ECOR systems at the Southern Great Plains central facility. We use ARM data to evaluate the measurements of $H$ and ET by the EBBR and ECOR methods. The ECOR measured $H$ may be accurate, while ET is substantially underestimated by ECOR [*Yang et al.*, 2004; *Asanuma et al.*, 2005; *Castellví et al.*, 2006; *Brunsell et al.*, 2008]. When both ECOR and EBBR data are available, the average $H/(R_n\text{-}G)$ are 0.475 (ECOR) and 0.487 (EBBR); and the average ET/$(R_n\text{-}G)$ are 0.303 (ECOR) and 0.477 (EBBR), as shown in Figure 5. The difference is greater in summer

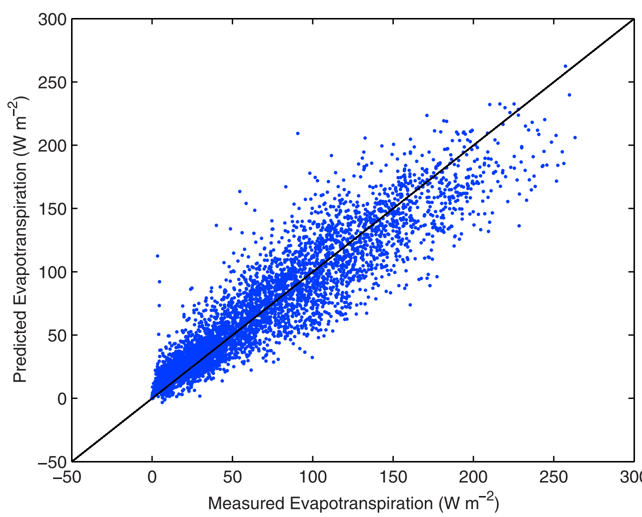


**Figure 3.** Comparison of the 16 day average predicted and ground-measured ET collected at all 64 sites shown in Table 1 when EVI is used. We used a 16 day average because the MODIS EVI data are available for a 16 day interval.

**Table 3.** Statistical Parameters of the Comparison Between the Measured and the Predicted 16 Day Averaged ET When EVI and NDVI are Used in Equations (8)–(10) During the Period Shown in Table 1[a]

| Site Name | EVI | | | NDVI | | |
|---|---|---|---|---|---|---|
| | Bias | STD | R | Bias | STD | R |
| KoFlux Gwangneung Supersite | −4.7 | 21.8 | 0.81 | −3.8 | 13.0 | 0.94 |
| KoFlux Haenam site | 11.6 | 22.6 | 0.93 | 11.3 | 18.0 | 0.92 |
| Mase paddy flux site | −3.2 | 14.2 | 0.95 | 5.4 | 18.0 | 0.95 |
| Tomakomai Flux Research Site | 7.2 | 21.9 | 0.89 | 8.5 | 18.5 | 0.93 |
| Kendall | 5.4 | 15.2 | 0.87 | 2.3 | 14.1 | 0.88 |
| Lucky Hills | 2.5 | 13.5 | 0.88 | −0.1 | 12.9 | 0.88 |
| Moshiri-Birch | 19.7 | 20.8 | 0.96 | 14.9 | 17.8 | 0.98 |
| Seto-Mixed | 4.2 | 17 | 0.94 | 9.8 | 11.8 | 0.97 |
| Howard Springs | −20.9 | 24.5 | 0.85 | −14.3 | 24.6 | 0.85 |
| Tumbarumba | −9.5 | 18.8 | 0.91 | 1.6 | 17.8 | 0.90 |
| Wallaby Creek Melbourne | −19.6 | 14 | 0.91 | −13.9 | 13.7 | 0.90 |
| Wallaby Creek canopy Melbourne | 1.9 | 7.4 | 0.97 | 8.0 | 11.0 | 0.97 |
| Maun Botswana Africa | −2.1 | 19.2 | 0.82 | −6.9 | 16.0 | 0.88 |
| British Columbia Campbell River | 10.4 | 15.5 | 0.95 | 14.6 | 18.2 | 0.95 |
| UCI - 1930 burn site Canada | 10.7 | 7.7 | 0.97 | 16.3 | 13.9 | 0.98 |
| UCI - 1850 burn site Canada | 14.4 | 10.2 | 0.98 | 21.2 | 18.6 | 0.98 |
| UCI - 1964 burn site Canada | 9.8 | 8.9 | 0.97 | 10.8 | 12.5 | 0.97 |
| UCI - 1981 burn site Canada | 9.6 | 9.4 | 0.97 | 13.3 | 13.5 | 0.98 |
| UCI - 1989 burn site Canada | 11.6 | 11.4 | 0.98 | 15.1 | 18.3 | 0.98 |
| UCI - 1998 burn site Canada | −0.6 | 7.7 | 0.97 | 4.7 | 9.3 | 0.97 |
| Seebodenalp Switzerland | −11.6 | 21.6 | 0.94 | −8.0 | 20.5 | 0.94 |
| Haibei China | 1.6 | 11.8 | 0.97 | −1.8 | 12.2 | 0.97 |
| Hillsboro, Kansas: EF02 | −4.3 | 22.3 | 0.95 | −5.5 | 21.2 | 0.95 |
| Plevna, Kansas: EF04 | 5.8 | 8.6 | 0.98 | 5.7 | 9.1 | 0.98 |
| Elk Falls, Kansas: EF07 | 1.1 | 18.1 | 0.95 | 1.5 | 17.7 | 0.96 |
| Coldwater, Kansas: EF08 | 0.2 | 16.4 | 0.91 | −1.5 | 16.6 | 0.9 |
| Ashton, Kansas: EF09 | −5.6 | 24.1 | 0.9 | −7.9 | 22.7 | 0.92 |
| Pawhuska, Oklahoma: EF12 | 8.9 | 15.5 | 0.98 | 9.8 | 14.9 | 0.98 |
| Lamont, Oklahoma: EF13 | −1.2 | 23.2 | 0.92 | −5.1 | 22.4 | 0.93 |
| Ringwood, Oklahoma: EF-15 | 5.3 | 10.8 | 0.97 | 2.3 | 11.5 | 0.97 |
| Morris, Oklahoma: EF-18 | 4.4 | 18.1 | 0.95 | 1.2 | 16.6 | 0.96 |
| El Reno, Oklahoma: EF-19 | 5.7 | 15.6 | 0.97 | 1.7 | 14.7 | 0.97 |
| Meeker, Oklahoma: EF-20 | 2.2 | 15.6 | 0.96 | 1.1 | 15.0 | 0.96 |
| Cordell, Oklahoma: EF-22 | −8.9 | 22.9 | 0.87 | −12.0 | 23.2 | 0.88 |
| Cement, Oklahoma: EF26 | 1.6 | 22.1 | 0.88 | −1.3 | 21.5 | 0.89 |
| Earlsboro, Oklahoma:EF27 | −0.2 | 14.9 | 0.96 | −0.9 | 14.8 | 0.96 |
| Palangkaraya | −0.8 | 20.3 | 0.91 | 3.7 | 29.0 | 0.88 |
| Tomakomai National Forest | −1.8 | 17.2 | 0.91 | −1.1 | 14.0 | 0.94 |
| Ivotuk | 14.8 | 20.9 | 0.85 | 10.1 | 18.8 | 0.85 |
| Audubon Research Ranch | −10.3 | 13.8 | 0.92 | −8.7 | 14.2 | 0.93 |
| Kendall Grasslands | −12.9 | 12.6 | 0.88 | −10.6 | 12.3 | 0.91 |
| Santa Rita Mesquite | −18.5 | 13.3 | 0.94 | −17.8 | 15.2 | 0.95 |
| Bonanza creek 1987 burn Delta | −2.4 | 9.3 | 0.99 | −1.0 | 7.5 | 0.99 |
| Bonanza creek 1999 burn Delta Junction | −2.2 | 10.7 | 0.93 | −1.3 | 10.5 | 0.94 |
| Bonanza creek control Delta Junction | −4.9 | 8.2 | 0.97 | −4.0 | 8.3 | 0.97 |
| Goodwin Creek | 12.4 | 21.7 | 0.93 | 10.9 | 20.5 | 0.93 |
| Fermi Laboratory (agricultural) Batavia | −0.2 | 15.5 | 0.97 | −5.4 | 15.9 | 0.97 |
| Fermi Laboratory (prairie) Batavia | −10.3 | 21.8 | 0.97 | −14.6 | 23.2 | 0.97 |
| Bondville | 2.5 | 23.6 | 0.94 | −1.9 | 21.1 | 0.94 |
| Kennedy Space Center (scrub oak) | 0.4 | 21.5 | 0.85 | 2.1 | 19.9 | 0.88 |
| Mead irrigated continuous maize | −5.2 | 24.5 | 0.97 | −9.5 | 24.6 | 0.97 |
| Mead irrigated maize-soybean rotation | −3.9 | 24.4 | 0.95 | −7.8 | 23.7 | 0.96 |
| Mead - rainfed maize-soybean rotation | −1.1 | 19.1 | 0.96 | −6.5 | 19.5 | 0.97 |
| Metolius - intermediate aged ponderosa pine | 2.6 | 12.6 | 0.92 | 8.6 | 13.9 | 0.91 |
| Ozark | 3.5 | 24.4 | 0.95 | −0.8 | 22.4 | 0.96 |
| Niwot Ridge Forest | −17.8 | 20.2 | 0.94 | −13.6 | 13.3 | 0.96 |
| Brookings | −14.4 | 30.5 | 0.90 | −18.8 | 28.6 | 0.91 |
| Mize - slash pine (clear-cut 3-yr regen) | −4.2 | 20.0 | 0.84 | −1.9 | 18.6 | 0.86 |
| Donaldson - slash pine (mid-rotation 12 yrs) | 1.5 | 17.2 | 0.88 | 7.0 | 16.9 | 0.90 |
| Walker Branch Watershed | 9.7 | 25.2 | 0.92 | 7.3 | 24.6 | 0.93 |
| Freeman Ranch mesquite juniper | 8.3 | 13.8 | 0.94 | 8.9 | 15.3 | 0.93 |
| Walnut River Watershed | −1.8 | 10.2 | 0.99 | −3.5 | 10.1 | 0.99 |
| Park Falls/WLEF | 8.5 | 16.2 | 0.94 | 4.5 | 17.0 | 0.93 |
| Willow Creek | 21.3 | 23.0 | 0.95 | 19.7 | 23.2 | 0.95 |
| Average | 0.6 | 17.1 | 0.93 | 0.8 | 17.0 | 0.94 |

[a]The bias (W $m^{-2}$), standard deviation (STD, W $m^{-2}$), and correlation coefficient (R) are shown.

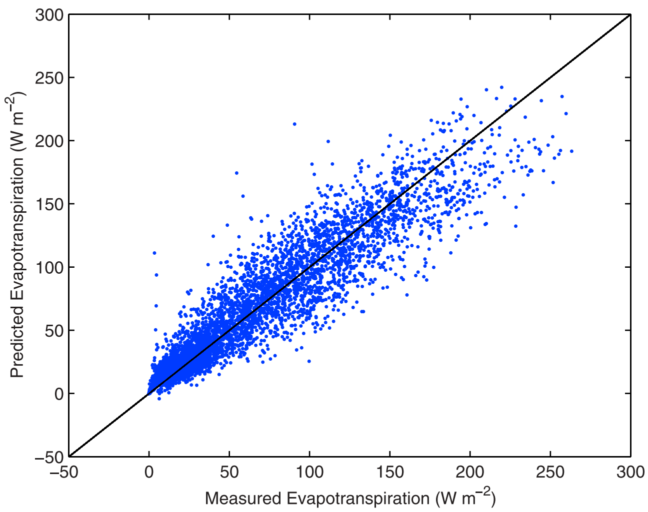


**Figure 4.** Comparison of the 16 day average predicted and ground-measured ET collected at all 64 sites shown in Table 1 when NDVI is used.

when ET is larger and ET/($R_n$-$G$) is near unity. Thus our use of *Twine et al.* [2000] to correct ET measured by the ECOR method may bias $H$ high and ET low (Figure 4). Data obtained from ET measurements also depend on the data processing methods [*Brunsell et al.*, 2008; *Wolf et al.*, 2008; *Haslwanter et al.*, 2009]. Table 3 shows that the proposed method overestimates ET at the UCI burned sites (Canada). The major reason for this is that the underestimation of ET measurement collected by ECOR method is not corrected because we are lack soil heat fluxes measurement to do the correction at the sites. The standard deviations and correlation coefficients at the sites are very good (Table 3), which indicate the proposed method works well.

[25] Figures 3 and 4 and Table 3 demonstrate the ability of the method to predict seasonal variation in ET accurately. To evaluate the ability of the method to predict the spatial variation in ET, we average the measured and predicted ET at each site over the entire period as shown in Table 1. Because the sites have different land cover types and different climate regimes, the comparison of the site-averaged ET demonstrates the ability of the method to predict the spatial variation in ET, as shown in Figure 6. The standard deviation of the comparison is 9.5 W m$^{-2}$ (14.2%) for NDVI and 9.3 W m$^{-2}$ (13.8%) for EVI. The correlation coefficients are 0.93 for either EVI or NDVI being used in equations (8)–(10).

[26] To evaluate how well the model predicts long-term variations in ET, we first average the predicted and measured ET data into annual bins for each site, and then remove the multiyear average from the annual values for each site to calculate the annual ET anomaly for every site. We only used

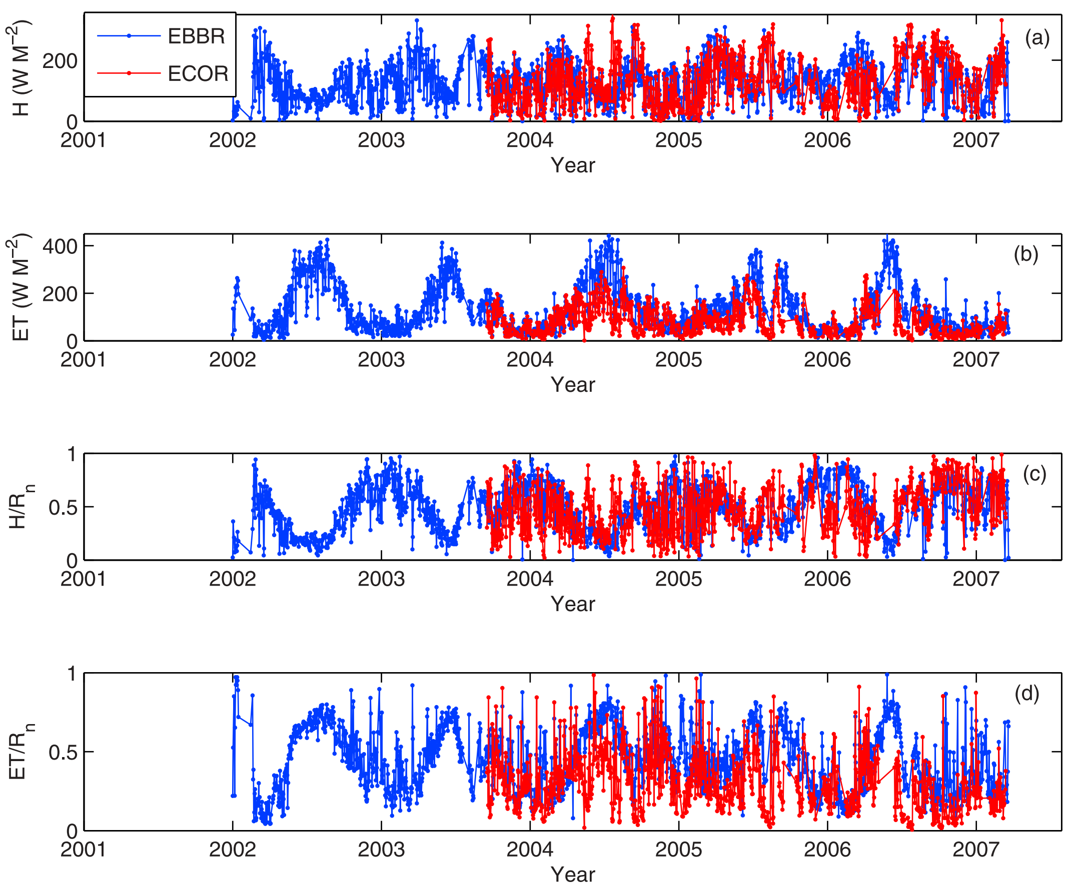


**Figure 5.** Comparison of the time series of ET and $H$ and their ratios to net radiation ($R_n$) collected by the Energy Balance Bowen Ratio (EBBR) and Eddy COVariance (ECOR) methods at the ARM Project central facility over the Southern Great Plains. The distance between these systems is about 0.2 km and both sites have the same type of pasture and wheat cover.

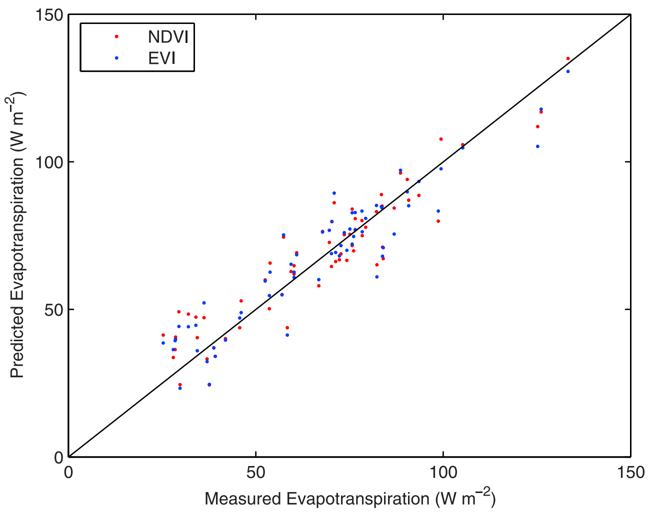


**Figure 6.** Comparisons of the predicted and measured site-averaged ET at 64 sites when EVI and NDVI are used. The proposed method overestimates ET when ET is low. This majorly occurs at the UCI burned sites (Canada, Tables 1 and 2). The major reason for this is that the underestimation of ET measurement collected by ECOR method (e.g., shown in Figure 4) is not corrected because we are lack soil heat fluxes measurement to do the correction at the sites. The standard deviations and correlation coefficients at the sites are good (Table 3), which indicate the proposed method works well at the sites.

sites where 5 years of data are available for this calculation. The results shown in Figure 7, demonstrate that the annual variation of ET is slightly larger than that expected, possibly due to missing ET data caused by bad weather conditions [*Falge et al.*, 2001]. We only used measurements of high-quality ET and without any gap filling. The correlation coefficient between the measured and predicted annual ET anomaly using NDVI is 0.82, with a standard deviation of 9.0 W m$^{-2}$ (7.4%) and when EVI is used, the correlation coefficient is 0.80, with a standard deviation of 9.4 W m$^{-2}$ (7.7%).

## 5. Conclusions

[27] The purpose of this paper is to develop a semiempirical method to obtain global estimates of ET on a multidecadal time scale. The method is developed to make use of data from ground-based tower sites those have collected ET data since the 1990s, and by themselves are too short and sparse to provide global multidecadal time series. This method adds empirical coefficients to a Penman like equation to include dependences on vegetation and soil moisture in order to be able to estimate ET over a wide range of climate conditions, using NDVI (satellite derived), $R_s$, $T_a$, WS, water vapor pressure deficit (VPD), and relative humidity deficit (RHD). It has low sensitivities to errors in the input data.

[28] The coefficients are derived by regression at 15 stations selected for the quality of their data and parameter coverage. The coefficients are validated with ground-based measurements at 49 additional stations. These data sets are the longest available, and provide continuous worldwide multisite measurements of ET, $R_s$, and corresponding meteorological observations, a total of 274 years. The sites are mainly located in North America and Asia, with the exception of three sites in Australia, two in Europe, and one in Africa. The climates of the sites vary from tropical to subarctic, and arid to humid. Site elevation ranges from near sea surface level to more than three thousand meters above sea level. The land cover types of the sites include desert grasslands, rainfed and irrigated croplands, grazed and ungrazed grasslands, savanna, shrub land, deciduous forest, evergreen forest and mixed forests.

[29] Validation tests assessed the ability of the derived method to reproduce seasonal, spatial, and interannual variability of ET. The seasonal and spatial variations in ET are accurately reproduced. The 16 day average daily ET can be estimated reasonably in terms of standard deviation and correlation coefficients. The method also improves estimates of the spatial variation in ET over previous methods and is also satisfactory in reproducing the interannual variability at sites with 5 years of data in both humid and arid regions. The correlation coefficient between measured and predicted annual ET anomalies using NDVI is 0.85. The 5 years of data used here alone does not allow us to distinguish longer time scale variability, e.g., decadal versus interannual.

[30] Only conventional measurements are required for our method, in particular, it avoids using SM to parameterize ET, a quantity that is currently not available at global and regional scales and has large spatial heterogeneity. It does not need near-surface gradients of air temperature and humidity. This simple but accurate method permits us to investigate the long-term variation in global ET over the land as will be demonstrated in part two of this paper series.

[31] This study uses RHD (1-RH/100) to parameterize the SM control on ET. Our analysis shows that RHD is closely correlated with SM of the surface layer (up to ~0.5 m depth), especially on a monthly scale. Thus RHD provides a nice quantitative index of the effect of soil moisture stress on ET, in particular during drought periods. The results of this paper show that the proposed model works well in predicting seasonal and annual variations of ET under different surface

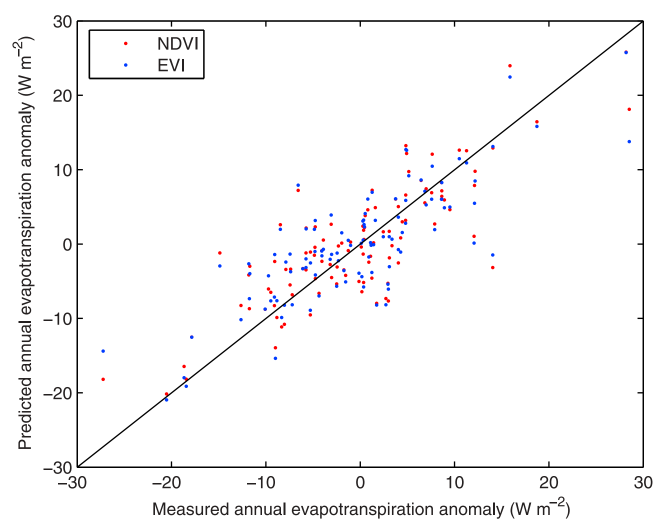


**Figure 7.** Comparison of the annual anomalies of predicted ET and ground-measured ET collected at the sites where 5 years of data are available (see Table 1).

aridity and land cover conditions using data measurements collected at globally distributed sites.

[32] The proposed model requires $R_s$, $T_a$, RH, WS, and VI as input data. $T_a$, RH and WS are observed at every weather station. VI is available through satellite observations from 1980s to present. $R_s$ directly observed since the 1958 at sparse points [*Wild*, 2009] and can also be derived from satellite cloud observations. $R_s$ can also be derived from other cloud and aerosol observations, including ground-based manual visual assessment by meteorological technicians, and sunshine duration measurements that have been observed in the last hundred years.

[33] In the second part, we will show how the method can be used with meteorological and satellite observations to determine regional and global variation of ET over the last 2 decades and what caused the variation. Input data are from meteorological observations of $T_a$, RH and WS, NOAA/AVHRR NDVI, direct measured $R_s$ collected by Global Energy Balance Archive (GEBA) and Sunshine duration derived $R_s$ to estimate climate variability over global-distributed 1120 stations from 1982 to 2002. The proposed model is found to work well in predicting climate variability of ET in different dry-wet conditions from deserts to tropical humid regions. Long-term variations of ET in humid areas such as the tropics, Europe and humid areas of Asia are primarily controlled by $R_s$ [*Wang et al.*, 2010]. However, soil water supply, is the dominant factor in controlling long-term variations of ET in arid areas [*Wang et al.*, 2010].

[34] **Acknowledgments.** The ET measurements of the Atmospheric Radiation Measurement (ARM) Project of the U.S. Department of Energy are downloaded from http://www.arm.gov/. Other ET measurements are downloaded from project websites including Ameriflux (http://public.ornl.gov/ameriflux/data-access.shtml), Asiaflux (http://asiaflux.yonsei.kr/index.html), FLUXNET (http://daac.ornl.gov/FLUXNET/), and the long-term carbon dioxide and water flux database (http://www.tucson.ars.ag.gov/dap/). We would like to thank the following principal investigators (email addresses in parentheses) for supplying their ET measurements to validate our modified Penman-Monteith method: Joon Kim (joon-kim@yonsei.ac.kr), Akira Miyata (amiyata@niaes.affrc.go.jp), Yasumi Fujinuma (fujinuma@nies.go.jp), William E. Emmerich (bill.emmerich@.ars.usda.gov), Takeshi (takeshi@agr.nagoya-u.ac.jp), Jason Beringer (jason.beringer@arts.monash.edu.au), Ray Leuning (Ray.Leuning@csiro.au), Musa Kilinc (Musa.Kilinc@arts.monash.edu.au), Elmar Veenendaal (Elmar.Veenendaal@wur.nl), T. (Andy) Black (andrew.black@ubc.ca), Michael Goulden (mgoulden@uci.edu), Nele Rogiers (nele.rogiers@psi.ch), Zhao Xinquan (xqzhao@mail.nwipb.ac.cn), Takashi Hirano (hirano@env.agr.hokudai.ac.jp), Walter Oechel (oechel@sunstroke.sdsu.edu), Tilden Meyers (tilden.meyers@noaa.gov), Russell Scott (sdmiller@uci.edu), James T. Randerson (jranders@uci.edu), Roser Matamala (matamala@anl.gov), Bert Drake (drakeb@si.edu), Shashi Verma (sverma1@unl.edu), Dean Vickers (vickers@coas.oregonstate.edu), Lianhong Gu (lianhong-gu@ornl.gov), Dean E. Anderson (deander@usgs.gov), Timothy Martin (tamartin@ufl.edu), Marcy Litvak (mlitvak@unm.edu), Richard Coulter (rlcoulter@anl.gov), Ken Davis (davis@essc.psu.edu), and Paul Bolstad (pbolstad@umn.edu). MODIS satellite data were obtained from https://wist.echo.nasa.gov/api/. The study is partially funded by NASA grant NNX08AC53G and National Research Program of China (2010CB950500). The upgrade of the Global Energy Balance Archive has been supported by the Swiss National Competence Center in Climate Research (NCCR climate). The work of the second author was supported by an NSF grant ATM- 0921898, and DOE grant DE-F602-01ER63198.

## References

Anderson, M. C., J. M. Norman, G. R. Diak, W. P. Kustas, and J. R. Mecikalski (1997), A two-source time-integrated model for estimating surface flux using thermal infrared remote sensing, *Remote Sens. Environ.*, *60*, 195–216, doi:10.1016/S0034-4257(96)00215-5.

Asanuma, J., H. Ishikawa, I. Tamagawa, Y. Ma, T. Hayashi, Y. Qi, and J. Wang (2005), Application of the band-pass covariance technique to portable flux measurements over the Tibetan Plateau, *Water Resour. Res.*, *41*, W09407, doi:10.1029/2005WR003954.

Baldocchi, D., et al. (2001), FLUXNET: A new tool to study the temporal and spatial variability of ecosystem-scale carbon dioxide, water vapor and energy flux densities, *Bull. Am. Meteorol. Soc.*, *82*, 2415–2434, doi:10.1175/1520-0477(2001)082<2415:FANTTS>2.3.CO;2.

Blyth, E. M., J. G. Evans, J. W. Finch, R. Bantges, and R. J. Harding (2006), Spatial variability of the English agricultural landscape and its effect on evaporation, *Agric. For. Meteorol.*, *138*, 19–28, doi:10.1016/j.agrformet.2006.03.007.

Brunsell, N. A., J. M. Ham, and C. E. Owensby (2008), Assessing the multi-resolution information content of remotely sensed variables and elevation for evapotranspiration in a tall-grass prairie environment, *Remote Sens. Environ.*, *112*, 2977–2987, doi:10.1016/j.rse.2008.02.002.

Burba, G. G., and S. B. Verma (2005), Seasonal and interannual variability in evapotranspiration of native tallgrass prairie and cultivated wheat ecosystems, *Agric. For. Meteorol.*, *135*, 190–201, doi:10.1016/j.agrformet.2005.11.017.

Castellví, F., A. Martínez-Cob, and O. Pérez-Coveta (2006), Estimating sensible and latent heat fluxes over rice using surface renewal, *Agric. For. Meteorol.*, *139*, 164–169, doi:10.1016/j.agrformet.2006.07.005.

Choudhury, B. J., N. U. Ahmed, S. B. Idso, R. J. Reginato, and C. S. T. Daughtry (1994), Relations between evaporation coefficients and vegetation indices studied by model simulations, *Remote Sens. Environ.*, *50*, 1–17, doi:10.1016/0034-4257(94)90090-6.

Davies, J. A., and C. D. Allen (1973), Equilibrium, potential, and actual evaporation from cropped surfaces in southern Ontario, *J. Appl. Meteorol.*, *12*, 649–657, doi:10.1175/1520-0450(1973)012<0649:EPAAEF>2.0.CO;2.

Detto, M., N. Montaldo, J. D. Albertson, M. Mancini, and G. Katul (2006), Soil moisture and vegetation controls on evapotranspiration in a heterogeneous Mediterranean ecosystem on Sardinia, Italy, *Water Resour. Res.*, *42*, W08419, doi:10.1029/2005WR004693.

Dirmeyer, P. A., Z. Guo, and X. Gao (2004), Comparison, validation and transferability of eight multi-year global soil wetness products, *J. Hydrometeorol.*, *5*, 1011–1033, doi:10.1175/JHM-388.1.

Entin, J., et al. (1999), Evaluation of Global Soil Wetness Project soil moisture simulations, *J. Meteorol. Soc. Jpn.*, *77*, 183–198.

Falge, E., et al. (2001), Gap filling strategies for long term energy flux data sets, *Agric. For. Meteorol.*, *107*, 71–77, doi:10.1016/S0168-1923(00)00235-5.

Gao, X., and P. A. Dirmeyer (2006), A multimodel analysis, validation, and transferability study of global soil wetness products, *J. Hydrometeorol.*, *7*, 1218–1236, doi:10.1175/JHM551.1.

Gao, Z. (2005), Determination of soil heat flux in a Tibetan Plateau short grass prairie, *Boundary Layer Meteorol.*, *114*, 165–178, doi:10.1007/s10546-004-8661-5.

Granier, A., et al. (2007), Evidence for soil water control on carbon and water dynamics in European forests during the extremely dry year: 2003, *Agric. For. Meteorol.*, *143*, 123–145, doi:10.1016/j.agrformet.2006.12.004.

Hammerle, A., A. Haslwanter, U. Tappeiner, A. Cernusca, and G. Wohlfahrt (2008), Leaf area controls on energy partitioning of a temperate mountain grassland, *Biogeosciences*, *5*, 421–431, doi:10.5194/bg-5-421-2008.

Haslwanter, A., A. Hammerle, and G. Wohlfahrt (2009), Open-path vs. closed-path eddy covariance measurements of the net ecosystem carbon dioxide and water vapour exchange: A long-term perspective, *Agric. For. Meteorol.*, *149*, 291–302, doi:10.1016/j.agrformet.2008.08.011.

Huete, A., K. Didan, T. Miura, E. P. Rodriguez, X. Gao, and L. G. Ferreira (2002), Overview of the radiometric and biophysical performance of the MODIS vegetation indices, *Remote Sens. Environ.*, *83*, 195–213, doi:10.1016/S0034-4257(02)00096-2.

Jarvis, P. G. (1976), The interpretation of the variations in leaf water potential and stomatal conductance found in canopies in the field, *Philos. Trans. R. Soc. London, Ser. B*, *273*, 593–610, doi:10.1098/rstb.1976.0035.

Kalma, J. D., T. R. McVicar, and M. F. McCabe (2008), Estimating land surface evaporation: A review of methods using remotely sensed surface temperature data, *Surv. Geophys.*, *29*, 421–469, doi:10.1007/s10712-008-9037-z.

Komatsu, T. S. (2003), Toward a robust phenomenological expression of evaporation efficiency for unsaturated soil surfaces, *J. Appl. Meteorol.*, *42*, 1330–1334, doi:10.1175/1520-0450(2003)042<1330:TARPEO>2.0.CO;2.

Koster, R. D., and M. J. Suarez (1999), A simple framework for examining the interannual variability of land surface moisture fluxes, *J. Clim.*, *12*, 1911–1917, doi:10.1175/1520-0442(1999)012<1911:ASFFET>2.0.CO;2.

Li, S. G., et al. (2006), Energy partitioning and its biophysical controls above a grazing steppe in central Mongolia, *Agric. For. Meteorol.*, *137*, 89–106, doi:10.1016/j.agrformet.2006.03.010.

Min, Q., and B. Lin (2006), Remote sensing of evapotranspiration and carbon uptake at Harvard Forest, *Agric. For. Meteorol.*, *100*, 379–387.
Monteith, J. L. (1965), Evaporation and environment, *Symp. Soc. Exp. Biol.*, *19*, 205–224.
Mu, Q., M. Zhao, F. A. Heinsch, M. Liu, H. Tian, and S. W. Running (2007), Evaluating water stress controls on primary production in biogeochemical and remote sensing based models, *J. Geophys. Res.*, *112*, G01012, doi:10.1029/2006JG000179.
Nagler, P. L., J. Cleverly, E. Glenn, D. Lampkin, S. Huete, and Z. Wan (2005), Predicting riparian evapotranspiration from MODIS vegetation indices and meteorological data, *Remote Sens. Environ.*, *94*, 17–30, doi:10.1016/j.rse.2004.08.009.
National Research Council (2007), *Earth Science and Applications from Space: National Imperatives for the Next Decade and Beyond*, 400 pp., Natl. Acad. Press, Washington, D. C.
Oncley, S. P., et al. (2007), The energy balance experiment EBEX-2000. Part I: Overview and energy balance, *Boundary Layer Meteorol.*, *123*, 1–28, doi:10.1007/s10546-007-9161-1.
Parlange, M. B., W. E. Eichinger, and J. D. Albertson (1995), Regional scale evaporation and the atmospheric boundary layer, *Rev. Geophys.*, *33*(1), 99–124, doi:10.1029/94RG03112.
Penman, H. L. (1948), Natural evaporation from open water, bare soil and grass, *Proc. R. Soc. London, Ser. A*, *193*, 120–145, doi:10.1098/rspa.1948.0037.
Phillips, O. L., et al. (2009), Drought sensitivity of the Amazon rainforest, *Science*, *323*, 1344–1347, doi:10.1126/science.1164033.
Priestley, C. H. B., and R. J. Taylor (1972), On the assessment of surface heat fluxes and evaporation using large-scale parameters, *Mon. Weather Rev.*, *100*, 81–92, doi:10.1175/1520-0493(1972)100<0081:OTAOSH>2.3.CO;2.
Reichle, R. H., R. D. Koster, J. Dong, and A. A. Berg (2004), Global soil moisture from satellite observations, land surface models, and ground data: Implications for data assimilation, *J. Hydrometeorol.*, *5*, 430–442, doi:10.1175/1525-7541(2004)005<0430:GSMFSO>2.0.CO;2.
Robock, A., et al. (2003), Evaluation of the North American Land Data Assimilation System over the southern Great Plains during the warm season, *J. Geophys. Res.*, *108*(D22), 8846, doi:10.1029/2002JD003245.
Schaake, J. C., et al. (2004), An intercomparison of soil moisture fields in the North American Land Data Assimilation System (NLDAS), *J. Geophys. Res.*, *109*, D01S90, doi:10.1029/2002JD003309.
Schüttemeyer, D., C. Schillings, A. F. Moene, and H. A. R. de Bruin (2007), Satellite-based actual evapotranspiration over drying semiarid terrain in West Africa, *J. Appl. Meteorol. Climatol.*, *46*, 97–111, doi:10.1175/JAM2444.1.
Shuttleworth, W. J. (1993), Evaporation, in *Handbook of Hydrology*, edited by D. R. Maidment, chap. 4, pp. 4.1–4.53, McGraw-Hill, New York.
Shuttleworth, W. J. (2007), Putting the "vap" into evaporation, *Hydrol. Earth Syst. Sci.*, *11*, 210–244, doi:10.5194/hess-11-210-2007.
Timmermans, W. J., W. P. Kustas, M. C. Anderson, and A. N. French (2007), An intercomparison of the Surface Energy Balance Algorithm for Land (SEBAL) and Two-Source Energy Balance (TSEB) modeling schemes, *Remote Sens. Environ.*, *108*, 369–384, doi:10.1016/j.rse.2006.11.028.
Tucker, C. J., J. G. R. Townshend, and T. E. Goff (1985), African land-cover classification using satellite data, *Science*, *227*, 369–375, doi:10.1126/science.227.4685.369.
Twine, T., et al. (2000), Correcting eddy-covariance flux underestimates over a grassland, *Agric. For. Meteorol.*, *103*, 279–300, doi:10.1016/S0168-1923(00)00123-4.
Wagner, W., K. Scipal, C. Pathe, D. Gerten, W. Lucht, and B. Rudolf (2003), Evaluation of the agreement between the first global remotely sensed soil moisture data with model and precipitation data, *J. Geophys. Res.*, *108*(D19), 4611, doi:10.1029/2003JD003663.
Wang, K., and S. Liang (2008), An improved method for estimating global evapotranspiration based on satellite determination of surface net radiation, vegetation index, temperature, and soil moisture, *J. Hydrometeorol.*, *9*, 712–727, doi:10.1175/2007JHM911.1.
Wang, K., and S. Liang (2009), Estimation of surface net radiation from solar shortwave radiation measurements, *J. Appl. Meteorol. Climatol.*, *48*, 634–643, doi:10.1175/2008JAMC1959.1.
Wang, K., Z. Li, and M. Cribb (2006), Estimation of evaporative fraction from a combination of day and night land surface temperature and NDVI: A new method to determine the Priestley-Taylor parameter, *Remote Sens. Environ.*, *102*, 293–305, doi:10.1016/j.rse.2006.02.007.
Wang, K., P. Wang, Z. Li, M. Cribb, and M. Sparrow (2007), A simple method to estimate actual evapotranspiration from a combination of net radiation, vegetation index, and temperature, *J. Geophys. Res.*, *112*, D15107, doi:10.1029/2006JD008351.
Wang, K., R. E. Dickison, M. Wild, and S. Liang (2010), Evidence for decadal variation in global terrestrial evapotranspiration between 1982 and 2002: 2. Results, *J. Geophys. Res.*, *115*, D20113, doi:10.1029/2010JD013847.
Watts, C. J., et al. (2007), Changes in vegetation condition and surface fluxes during NAME 2004, *J. Clim.*, *20*, 1810–1820, doi:10.1175/JCLI4088.1.
Wild, M. (2009), Global dimming and brightening: A review, *J. Geophys. Res.*, *114*, D00D16, doi:10.1029/2008JD011470.
Wilson, K., et al. (2002), Energy balance closure at FLUXNET sites, *Agric. For. Meteorol.*, *113*, 223–243, doi:10.1016/S0168-1923(02)00109-0.
Wolf, A., N. Saliendra, K. Akshalov, D. A. Johnson, and E. Laca (2008), Effects of different eddy covariance correction schemes on energy balance closure and comparisons with the modified Bowen ratio system, *Agric. For. Meteorol.*, *148*, 942–952, doi:10.1016/j.agrformet.2008.01.005.
Yang, F., et al. (2006), Prediction of continental-scale evapotranspiration by combining MODIS and AmeriFlux data through support vector machine, *IEEE Trans. Geosci. Remote Sens.*, *44*, 3452–3461, doi:10.1109/TGRS.2006.876297.
Yang, K., T. Koike, and H. Ishikawa (2004), Analysis of the surface energy budget at a site of GAME/Tibet using a single-source model, *J. Meteorol. Soc. Jpn.*, *82*, 131–153, doi:10.2151/jmsj.82.131.

R. E. Dickinson and K. Wang, Department of Geological Sciences, University of Texas at Austin, Austin, TX 78712, USA. (kcwang@jsg.utexas.edu)

S. Liang, Department of Geography, University of Maryland, College Park, MD 20742, USA.

M. Wild, Institute for Atmospheric and Climate Science, ETH Zürich, CH-8092 Zürich, Switzerland.